Sensorless Control Strategy for Brushless DC Motor Drives Based on Sliding Mode Observer

Jalal Jamshidi and Hossein Tohidi
Department of Electrical Engineering, College of Engineering, Malekan Branch, Islamic Azad University, Malekan, Iran

Abstract
Brushless DC (BLDC) motors are widely used in a variety of applications such as industrial automation and electric vehicle (EV) appliances. Back electromotive force EMF is the only electric quantity able to provide instantaneous information on the mechanical variables of the BLDC motor; that is true for the position and speed. In this paper, an accurate Sliding Mode Observer of the trapezoidal back EMF is applied to the BLDC motor in order to ensure the control without speed and position sensors. A theoretical study is developed and the effectiveness of proposed control strategy has been validated by simulation results.

Keywords
Brushless DC (BLDC) motor, Electric vehicle (EV), Sensorless control, Sliding mode observer, Torque ripple.

1. Introduction

Permanent magnet brushless DC (BLDC) motors offer many advantages including high efficiency, low maintenance, greater longevity, reduced weight and more compact construction. The BLDC motors have been widely used for various industrial application based on inherent advantages. Today the demand for BLDC motor in the industrial, domestic, and electric vehicle (EV) applications is steadily rising. A BLDC motor is one kind of synchronous motor, having permanents magnets on the rotor and trapezoidal shape back EMF [1-3].

Conventional BLDC motor drives are generally implemented via a six-switch three-phase inverter, position and current sensors that generate proper signals for current commutation [4]. The most popular way to control BLDC motor is through the voltage source current-controlled inverters. The inverter must supply a rectangular current waveform, is proportional to the motor shaft torque. Three Hall Effect sensors are usually used as position sensors to perform current commutations; it is only required to know the position of commutation points, because the objective is to achieve rectangular current waveforms, with dead time periods of 60o. However, it is a well-known fact that these sensors have a great number of drawbacks; they increase the cost of the motor and require special mechanical arrangements to be mounted. Furthermore, sensorless control is the reliable way to operate the motor for applications in harsh environments [5].

In recent years, a lot of researches on sensorless control techniques of BLDC motors have been conducted. This research can be divided into four categories. 1) Detecting the zero crossing points of the motor terminal to neutral voltage with or without precise phase shift circuit [6]. 2) Back electromagnetic force (EMF) integration method [7]. 3) Sensing the third harmonic of the back EMF [8]. 4) Detecting the freewheeling diode conduction and related extensive strategies [9]. Among the various techniques, the back EMF zero crossing detection method is the most popular due to its simplicity, ease of implementation, and lower cost [10].

In other methods, the estimation of the instantaneous rotor position is proposed. In [11], the instantaneous rotor position of the BLDC motor is estimated indirectly from the estimating flux linkage using measured motor voltages and currents. The accuracy of the rotor position estimation depends significantly on the motor parameter variation. In [12], the Extended Kalman Filter is used to estimate the instantaneous rotor position and speed of the BLDC motor, but the speed estimation accuracy is decreased, particularly at low speeds.

In this paper, an accurate sensorless control strategy using a Sliding Mode Observer of the trapezoidal back EMF is proposed in order to ensure the control of the BLDC motor without speed and position sensors. The proposed control strategy is based on hysteresis current controllers and a PI controller for speed regulation. This control strategy represents an attractive proposal because it is robust with respect to measurements noise. The trapezoidal back EMF which will be observed is the back EMF, induced between two phases, which does not depend neither on the stator voltage harmonics of order multiple of three nor on the noise of commutation introduced by the inverter. It is largely sufficient to provide the six positions of commutation and the speed of the rotor. However the continual estimation for the rotor position becomes not necessary.

The organization of this paper is given hereafter. In section II, the BLDC motor operation principle is introduced. In section III, proposed sensorless control strategy is explained. This section contain the analysis of the proposed drive system, sliding mode observer, and rotor

Manuscript received December 5, 2016
Manuscript revised December 20, 2016

position and speed estimation. Finally, in section IV, the simulation results by MATLAB software are shown.

2. BLDC Motor Drive Operation Principal

The BLDC motor employs a DC power supply switched to the stator phase windings of the motor by power devices, the switching sequence being determined from the rotor position. The phase current of BLDC motor, in typically rectangular shape, is synchronized with the back EMF to produce constant torque at a constant speed Fig. 1 shows the structure of a six-switch three-phase BLDC motor. These motors are driven by a three-phase inverter with six-step commutation. The conducting interval for each phase is 120o electrical degree. Each conducting stage is called one step. Therefore, only two phases conduct current at anytime, leaving the third phase floating. In order to produce maximum torque, the inverter should be commutated every 60o so that current is in phase with the back EMF.

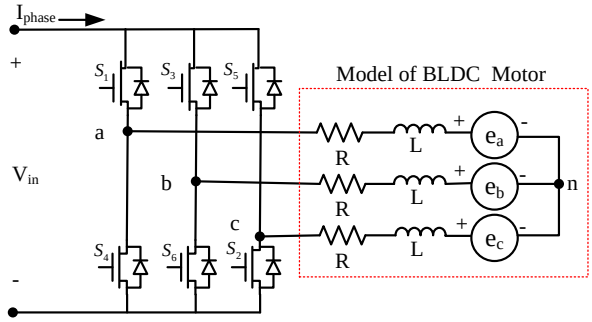

Fig. 1. The structure of BLDC motor drive

The typical mathematical model of the BLDC motor is described as:

$$\begin{bmatrix} v_{aN} \\ v_{bN} \\ v_{cN} \end{bmatrix} = \begin{bmatrix} R & 0 & 0 \\ 0 & R & 0 \\ 0 & 0 & R \end{bmatrix} \begin{bmatrix} i_a \\ i_b \\ i_c \end{bmatrix} + \begin{bmatrix} L & 0 & 0 \\ 0 & L & 0 \\ 0 & 0 & L \end{bmatrix} \frac{d}{dt} \begin{bmatrix} i_a \\ i_b \\ i_c \end{bmatrix} + \begin{bmatrix} e_a \\ e_b \\ e_c \end{bmatrix} \quad (1)$$

$$L = (L_S - L_M) \quad (2)$$

where v_{aN} represents the terminal phase a voltage with respect to the star point, i_a is the rectangular-shaped phase a current, e_a is the trapezoidal-shaped back EMF, and R, L_S and L_M are the resistance, self-inductance and mutual-inductance, respectively. The electromagnetic torque is expressed as:

$$T_e = \frac{1}{\omega_r}(e_a i_a + e_b i_b + e_c i_c) \quad (3)$$

where ω_r is the mechanical speed of the rotor and T_e is the electromagnetic torque. The equation of motion is:

$$\frac{d}{dt}\omega_r = (T_e - T_L - B\omega_r)/J \quad (4)$$

where B is the damping constant, J is the moment of inertia of the drive and TL is the load torque.

The commutation timing is determined by the rotor position, which can be detected by Hall sensors or estimated from motor parameters if it is sensorless system. For the three phases BLDC motor the phase to phase back EMFs and phase current waveforms are shown in Fig. 2.

In this paper, the position estimator is used to detect only six positions, which determine the switch commutations or commutations points (Fig. 2). From the outputs of the Sliding Mode Observer the phase to phase back EMFs are observed and using the zero crossing detectors (ZCD), the positions of commutation points are estimated. The rotor speed obtained by a new approach which based on the relation mathematical find between the magnitudes of the phase to phase back EMFs.

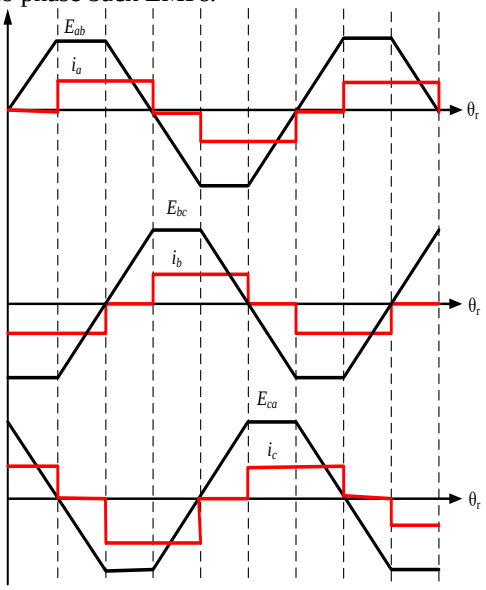

Fig. 2. Phase to phase Back EMFs and phases current waveforms

3. Proposed Sensorless Control Strategy

A. *Analysis of the Proposed Drive System*

In general, current control strategies for BLDC motor drives can be divided into three topologies: Hysteresis Band Control, PWM Control, and Variable DC-link Voltage Control. Hysteresis Band Control that used in this paper is one of the simplest closed-loop control schemes. In Hysteresis Band Control, the value of the controlled variable is forced to stay within certain limits (hysteresis band) around a reference value. Fig. 3 shows a schematic of the proposed control strategy. For control of speed and

armature currents of motor, first, the speed of the motor is compared with its reference value. The speed error can be represented as:

$$e_{\omega}(t) = \omega_{ref} - \omega_r(t) \quad (5)$$

where, ωref is the reference speed value and ωr(t) is the measured speed value at time t. The speed error is processed in the PI speed controller. The output of the speed controller is the reference torque value, but, According to this relation:

$$I_{ref} = T_{ref} / K_t \quad (6)$$

where, Tref and Kt are the reference torque and torque constant respectively, the output of speed controller is considered as the reference current (Iref). Then, the measured phase currents are compared with the reference currents. The input of the each current controllers is:

$$e_i(t) = I_{ref}(t) - I_{abc}(t) \quad (7)$$

From this comparison, current error signal ei(t) is obtained. This error passing through a simple hysteresis current controller directly generates chopping for all six power switches of the inverter. Ultimately the hysteresis current controller regulates the winding currents within the small band around the reference currents values.

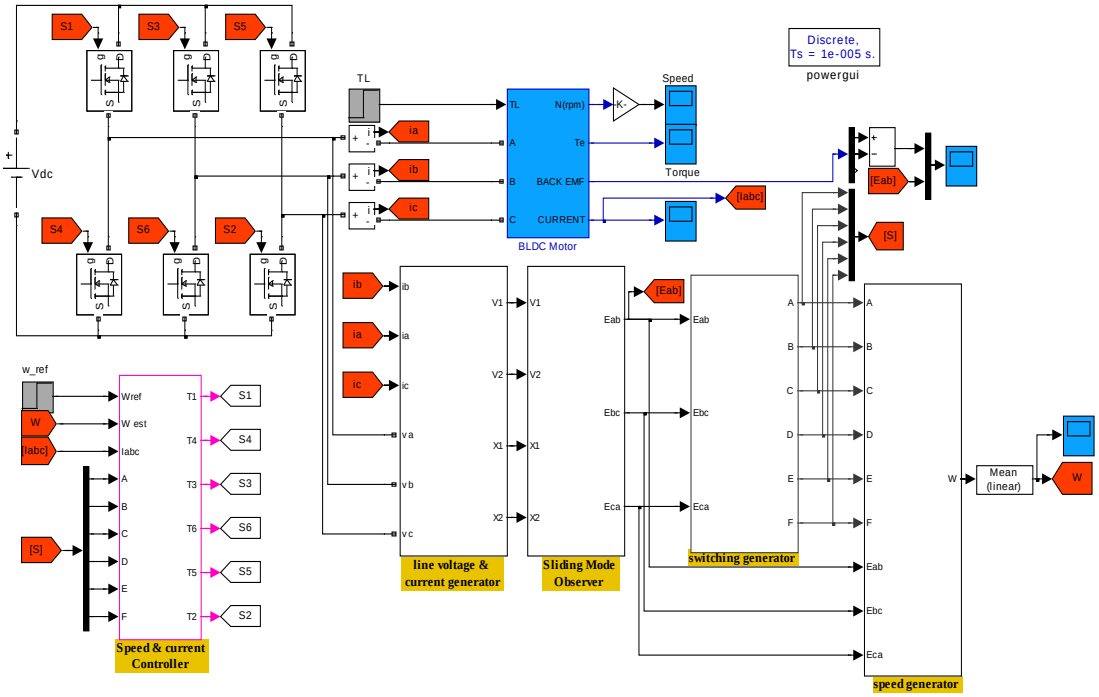

Fig. 3. Block diagram of proposed sensorless control strategies and drive system

B. *Sliding Mode Observer*

The observer presented in this paper is a very simple case of the Sliding Mode Observer. It is a linear model disturbed by the phase to phase back EMFs and the errors parametric. By using the measurements of the stator currents and the input phase to phase voltage, the objective is to observer the phase to phase back EMFs (Fig. 4). The first step is the modeling of BLDC motor in the stationary reference frame abc using the subtractions currents (Ia-Ib, Ib-Ic, Ic-Ia) which measured through stator phases, the phase to phase back EMFs (Eab, Ebc, Eca) and the phase to phase voltages (Uab, Ubc, Uca). The following model has been derived:

$$\begin{cases} \dfrac{d(I_a - I_b)}{dt} = -\dfrac{R}{L}(I_a - I_b) - \dfrac{1}{L}E_{ab} + \dfrac{1}{L}U_{ab} \\ \dfrac{d(I_b - I_c)}{dt} = -\dfrac{R}{L}(I_b - I_c) - \dfrac{1}{L}E_{bc} + \dfrac{1}{L}U_{bc} \\ \dfrac{d(I_c - I_a)}{dt} = -\dfrac{R}{L}(I_c - I_a) - \dfrac{1}{L}E_{ca} + \dfrac{1}{L}U_{ca} \end{cases} \quad (8)$$

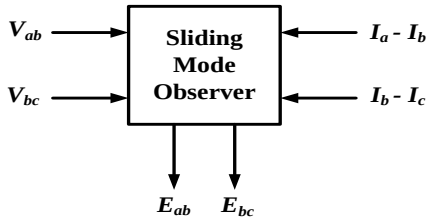

Fig. 4. Sliding mode observer

To reduce the order of the Eq. 8, only the electric quantities of the two phases (a-b) respectively (b-c) are taken. The following traditional assumptions are made:

- The distribution of the phase to phase back EMF is trapezoidal, and its variation is very slow.
- The motor is unsaturated.
- The armature reaction **is** negligible

The model in Eq. 8 can rewritten as follows:

$$\begin{cases} \frac{d(I_a - I_b)}{dt} = -\frac{R}{L}(I_a - I_b) - \frac{1}{L}E_{ab} + \frac{1}{L}U_{ab} \\ \frac{d(I_b - I_c)}{dt} = -\frac{R}{L}(I_b - I_c) - \frac{1}{L}E_{bc} + \frac{1}{L}U_{bc} \\ \frac{dE_{ab}}{dt} = 0 \\ \frac{dE_{bc}}{dt} = 0 \end{cases} \quad (9)$$

Assuming the simplified model of Eq. 9 the vector of state $x = ((I_a - I_b), (I_b - I_c), E_{ab}, E_{bc})^T$, and the input vector $v = (U_{ab} - U_{bc})$, the Sliding Mode Observer can be easily described in the following form:

$$\begin{cases} \hat{x}_1' = -\alpha_1 x_1 - \alpha_2 \hat{x}_3 + \alpha_2 V_1 + K_1 I_s \\ \hat{x}_2' = -\alpha_1 x_2 - \alpha_2 \hat{x}_4 + \alpha_2 V_2 + K_2 I_s \\ \hat{x}_3' = K_3 I_s \\ \hat{x}_4' = K_4 I_s \end{cases} \quad (10)$$

Where $\alpha_1 = \frac{R}{L}$, $\alpha_2 = \frac{1}{L}$ and $K_1 = (k_{11}, k_{12})$, $K_2 = (k_{21}, k_{22})$, $K_3 = (k_{31}, k_{32})$, $K_4 = (k_{41}, k_{42})$

Are the gains of Sliding Mode Observer. The sliding surface S is given by:

$$S = \begin{bmatrix} x_1 - \hat{x}_1 \\ x_2 - \hat{x}_2 \end{bmatrix} = \begin{bmatrix} S_1 \\ S_2 \end{bmatrix} = \begin{bmatrix} 0 \\ 0 \end{bmatrix}, \quad I_s = \begin{bmatrix} sign(s_1) \\ sign(s_2) \end{bmatrix} \quad (11)$$

By define the tracking errors as $e = x - \hat{x}$, its dynamic is governed by:

$$\begin{cases} e_1' = -\alpha_2 e_3 - K_1 I_s \\ e_2' = -\alpha_2 e_2 - K_2 I_s \\ e_3' = -K_3 I_s \\ e_4' = -K_4 I_s \end{cases} \quad (12)$$

In order to ensure the asymptotic convergence of the tracking errors e to zero, the K gains should properly adjusted.

C. Rotor Position and Speed Estimation

From the phase to phase back EMF (Fig. 2), the detection of six positions of the rotor can be determined easily, by using a zero crossing detectors (ZCD) of this phase to phase back EMF. For example, during the switch commutation phase *a* of the transistor S_1, one can deduce that the phase to phase back EMF E_{ab} is always positive and that the phase to phase back E_{ca} is always negative, this is mean that it is possible to obtain a sufficient condition to extract the state switch commutation phase *a* of the transistor S_1 : it is thus enough to have $(E_{ab} > 0, E_{ca} < 0)$. For the other switch commutations the same logic of analysis is followed. Therefore, a digital circuit can be easily developed as Fig. 5.

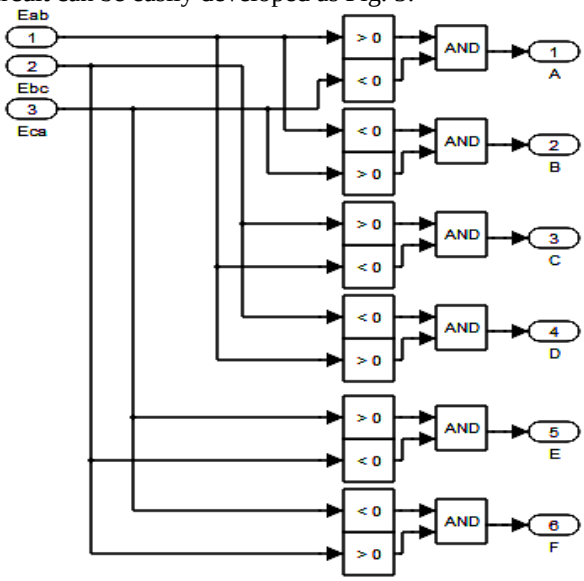

Fig. 5. The zero crossing detector circuit

For the application of the sensorless drives in which high estimation accuracy of rotor speed is required, the Extended Kalman Filter has been used to obtain the instantaneous position and speed. According the drawbacks mentioned previously, the objective of this paper is to use only the Sliding Mode Observer. Then a new method is used, which based on the relation mathematical between the magnitudes of phase to phase back EMF and speed error. The rotor speed can be estimated using only the magnitude phase to phase back EMF tacking by Sliding Mode Observer.

$$\omega_r = \frac{E_{\max(phase-to-phase)}}{2K_{EMF}} \quad (13)$$

With

$$E_{\max(phase-to-neutral)} = K_{EMF}\omega_r \quad (14)$$

$$E_{\max(phase-to-neutral)} = \frac{E_{\max(phase-to-phase)}}{2} \quad (15)$$

Where K_{EMF} is the constant of the back EMF.

A logical circuit (Fig. 6) is developed using the phase to phase back EMF observed by sliding mode observer and the six points of commutations determined through the circuit digital of detection de switch commutations (Fig. 5).

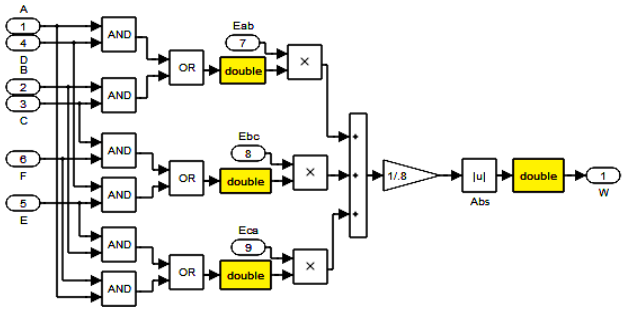

Fig. 6. The rotor speed detector circuit

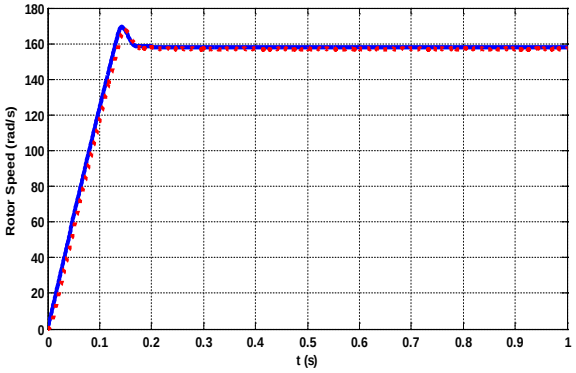

Fig. 8. Actual and estimated speed of BLDC motor.

4. Simulation Results

To evaluate the performance of the proposed drive system, simulation models have been established using MATLAB/SIMULINK. The main parameters of BLDC motor are listed in Table I. The sampling interval is 10μsec, the magnitude of the current hysteresis band is 0.2A.

TABLE I Simulation parameters of the BLDC motor

Parameters	Value
Phase resistance	0.4 Ω
Phase inductance	13 mH
Rated speed	1500 rpm
DC link voltage	300 V
Pole pairs	1
Rated torque	3 N.m
Inertia	0.004 kg.m^2
Torque constant	0.4 V/(rad/sec)

Actual (solid blue curve) and estimated (dashed red curve) phase to phase Eab back EMF of BLDC motor are depicted in Fig. 7. As Fig. 7 shows, the phase to phase back EMF follows closely the ideal trapezoidal phase to phase back EMF of the motor and this verify the well control capability of BLDC motor by proposed sliding mode observer. Actual (solid blue curve) and estimated (dashed red curve) motor speed are illustrated in Fig. 8. In the response of the sliding mode observer, the speed observed follow the same measured speed.

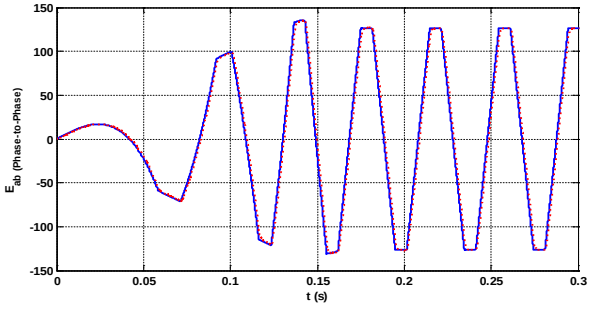

Fig. 7. Actual and estimated phase to phase Eab back EMF of BLDC motor.

Fig. 9 shows the BLDC motor operation at rated speed 1500 rpm (157 rad/s) and rated torque 3 N.m. According to Fig. 9(a,b), it is clear that speed tracking is well and the developed torque has low ripple. Moreover the current waveforms are the same as quasi-square waveforms with low ripples.

As mentioned before, BLDC motors are widely used in electric vehicle applications as traction electric drive. Electric vehicle traction drives have different operation conditions with variable speed and torque. The speeds of motor at variable speed condition is depicted in Fig. 10. As Fig. 10 shows, the motor speed follow the reference speed, and this verify that the proposed drive system can operate successfully in electric vehicle applications.

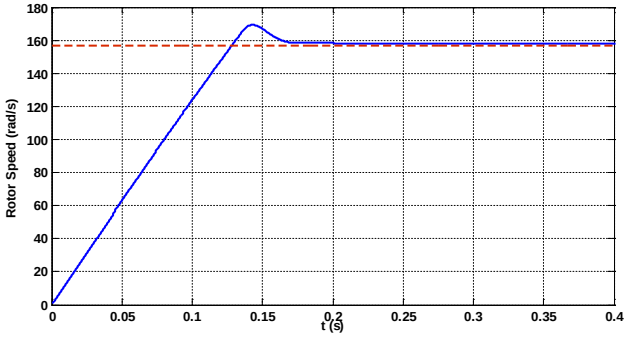

(a)

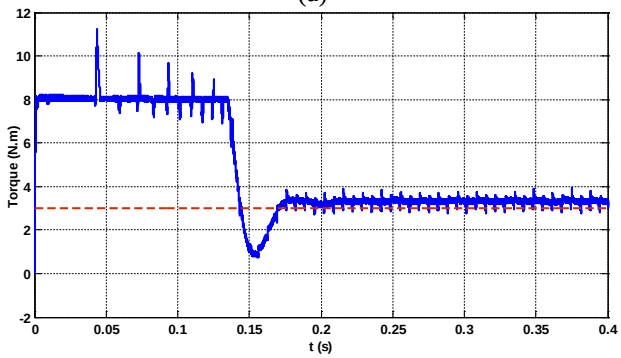

(b)

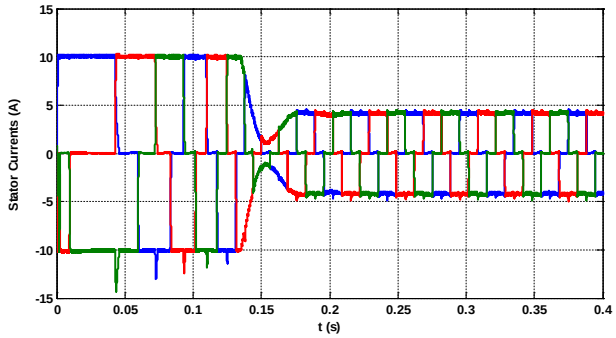

(c)

Fig. 9. Proposed drive responces at reated speed and full load condition. (a) speed, (b) developed electromagnetic torque, (c) phase current waveforms.

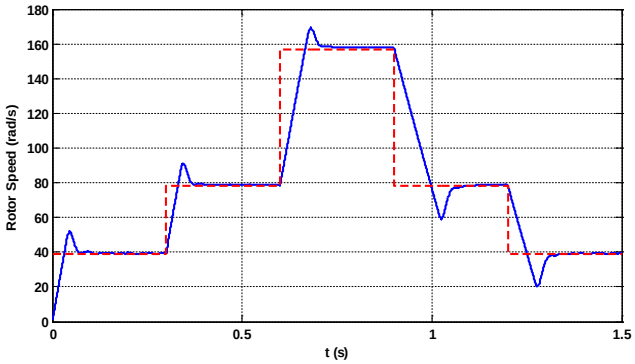

Fig. 10. The speeds of motor at variable speed condition.

5. Conclusion

A higher performance BLDC motor drive system has been proposed. Using the presented method, which applied the Sliding Mode Observer, the speed and rotor position of the BLDC motor are estimated from the phase to phase back EMF. The results obtained by simulation show the effectiveness of the method. The proposed strategy makes possible low cost industrial appliances using BLDC motor, such as electric vehicle, to obtain the good sound quality.

References

[1]. G. Liu, C. Cui, K. Wang, B. Han and S. Zheng, "Sensorless Control for High-Speed Brushless DC Motor Based on the Line-to-Line Back EMF," in *IEEE Transactions on Power Electronics*, vol. 31, no. 7, pp. 4669-4683, July 2016.

[2]. R. Kumar and B. Singh, "BLDC Motor-Driven Solar PV Array-Fed Water Pumping System Employing Zeta Converter," in *IEEE Transactions on Industry Applications*, vol. 52, no. 3, pp. 2315-2322, May-June 2016.

[3]. A. Darba, F. De Belie, P. D'haese and J. A. Melkebeek, "Improved Dynamic Behavior in BLDC Drives Using Model Predictive Speed and Current Control," in *IEEE Transactions on Industrial Electronics*, vol. 63, no. 2, pp. 728-740, Feb. 2016.

[4]. P. Pillay, R. Krishnan; "Modeling, simulation, and analysis of permanent-magnet motor drives. II: The Brushless DC Motor Drive", IEEE Trans. Ind. Appl., vol. 25, no. 2, pp. 274-279, Mar/Apr 1989.

[5]. H. Li, S. Zheng and H. Ren, "Self-Correction of Commutation Point for High-Speed Sensorless BLDC Motor With Low Inductance and Nonideal Back EMF," in *IEEE Transactions on Power Electronics*, vol. 32, no. 1, pp. 642-651, Jan. 2017.

[6]. A. H. Niasar, A. Vahedi, and H. Moghbeli, "A novel position sensorless control of a four-switch, brushless DC motor drive without phase shifter," IEEE Trans. Power Electron., vol. 23, no. 6, pp. 3079–3087, Nov. 2008.

[7]. R. C. Becerra, T. M. Jahns, and M. Ehsani, "Four-quadrant sensorless brushless ECM drive," in Proc. APEC'91, 1991, pp. 202–209.

[8]. J. Moreira, "Indirect sensing for rotor flux position of permanent magnet AC motors operating over a wide speed range," IEEE Trans. Ind. Appl., vol. 32, no. 6, pp. 1394–1401, Nov./Dec. 1996.

[9]. S. Ogasawara and H. Akagi, "An approach to position sensorless drive for brushless dc motors," IEEE Trans. Ind. Appl., vol. 27, no. 5, pp. 928–923, Sep./Oct. 1991.

[10].G. J. Su and W. McKeever, "Low-cost sensorless control of brushless DC motors with improved speed range," IEEE Trans. Power Electron., vol. 19, no. 2, pp. 296–302, Mar. 2004.

[11].S. Bejerke, "Digital signal processing solutions for motor control using the TMS320F240DSP-controIler", ESIEE, Paris, September, 1996.

[12].B. Terzic, and M. Jadric,"Design and Implementation of the Extended Kalman Filter for the Speed and Rotor Position Estimation of Brushless DC Motor" IEEE Trans, on Industrial Electronics, Vol. 48, No. 6, Dec. 2001.